NONLINEAR INTERACTIONS BETWEEN A FREE SURFACE FLOW WITH SURFACE TENSION AND A SUBMERGED CYLINDER

Roger Matsumoto Moreira
School of Engineering, Fluminense Federal University
R. Passos da Pátria 156, bl.D, sl.505, Niterói, R.J., Brazil.
CEP: 24210-240. E-mail: rmmoreira@engenharia.uff.br

Abstract.*A submerged cylinder in a uniform stream flow is approximated by a horizontal doublet, following Lamb's classical method. Surface tension effects and a dipole are included in the fully nonlinear, unsteady, non-periodic, boundary-integral solver described by Tanaka et al. (1987). Nonlinear effects are modelled by considering a linear stationary solution as an initial condition for the fully nonlinear irrotational flow program. These unsteady flows approach a steady solution for some parameters after waves have radiated away. In other cases the flow does not approach a steady solution. These cases are of interest and are discussed.*

Keywords*. Potential flow, nonlinear effects, capillary effects, boundary integral method.*

1. Introduction

Surface waves are generated when water flows past obstacles or when ships move over the surface. Interesting features at the free surface can be observed due to these interactions, with gravity and, on a smaller scale, surface tension acting as the restoring forces. Modelling these phenomena with the inclusion of nonlinearity and surface tension effects helps to understand the resulting free surface flow. The knowledge of these wave phenomena has great practical significance, being an important factor in the design of ships and offshore structures such as oil rigs, or in the study of sediment transport around coasts.

In this context the study of disturbances produced at a free surface by the flow of a uniform stream interacting with a submerged cylinder has attracted the interest of researchers since the early 20th century. Kelvin was perhaps the first to suggest that problem in 1905, followed by Lamb who analysed it formally in the light of linear water wave theory in 1913 (for a more accessible version of this paper see Lamb 1932, §247). In Lamb's classical method, a submerged cylinder in a uniform stream flow is approximated by a horizontal doublet. For a steady irrotational potential flow with a linearised free surface boundary condition, Lamb found the appearance of a local disturbance immediately above the obstacle, followed by a train of stationary sinusoidal waves on the downstream side (see figure 1a).

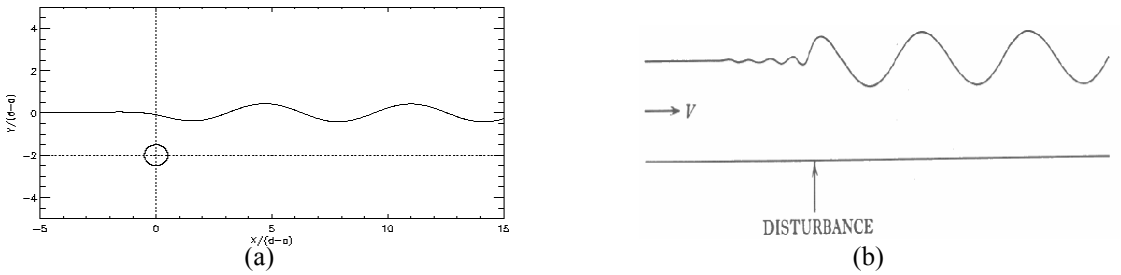

Figure 1. (a) Stationary waves due to the presence of a cylinder on a uniform stream flow. (b) A sketch of the capillary and "gravity-like" waves produced by a steady disturbance on a uniform stream flow.

Investigations on the importance of nonlinear effects from the free surface boundary condition were carried out later. Tuck (1965) introduced nonlinear second-order corrections to Lamb's first-order linearised solution, suggesting that the exact nonlinear solution would involve highly non-sinusoidal or even breaking waves. Dagan (1971) investigated the same problem by the method of matched asymptotic expansions at high Froude numbers. A good agreement with linear theory was found for deep submerged bodies, while for a body close to the free surface the nonlinear calculations differed significantly from the linearised solution.

By assuming that the waves are sufficiently small, a linear steady solution including surface tension effects can be derived, showing that under certain conditions small-scale ripples are formed ahead of the cylinder, while a train of "gravity-like" waves appear downstream (see figure 1b). To investigate the effects of surface tension and nonlinearity at the free surface when a horizontal submerged cylinder meets a stream flow, a dipole is included in the fully nonlinear, unsteady, non-periodic, boundary-integral solver described by Tanaka *et. al.* (1987). Nonlinear effects are modelled with the linear stationary solution as the initial condition for the fully nonlinear irrotational flow program. These unsteady flows approach a steady solution for some parameters after waves have radiated away. In other cases the flow does not approach a steady solution. These cases are of special interest and are discussed.

2. Boundary value problem

The fluid flow is assumed to be inviscid and incompressible while surface tension effects are included in the model. The singularity, a single doublet, is positioned below the free surface and interacts with a constant horizontal stream velocity U. It is assumed that the flow is irrotational outside the singular core and away from the free surface. The irrotational velocity field $\vec{u}(x,y,t)$ is then given by the gradient of a full velocity potential $\Phi(x,y,t)$ which satisfies Laplace's equation in the fluid domain, excluding the singular point,

$$\nabla^2 \Phi = 0 . \tag{1}$$

From Green's theorem all the interior properties of the fluid can be determined by its properties at the boundaries alone. The entire motion can then be modelled by considering a point discretisation of the surface. The velocity of the fluid at the surface is determined using,

$$\vec{u} = \nabla \Phi = \frac{\partial \Phi}{\partial n_1} \vec{n}_1 + \frac{\partial \Phi}{\partial n_2} \vec{n}_2 , \tag{2}$$

where $\vec{n}_1$ and $\vec{n}_2$ are the tangential and normal unit vectors respectively.

The introduction of the dipole in our model is done by decomposing our full velocity potential Φ into a regular part ϕ_w (due to surface waves) and a singular part ϕ_s (due to the doublet),

$$\Phi = \phi_w + \phi_s, \tag{3}$$

which satisfies Laplace's equation. The kinematic boundary condition to be satisfied at the free surface is based on a continuum idea that a fluid particle described by a position vector $\vec{r}(x,y,t)$ on the moving free surface remains on it. Therefore,

$$\frac{D\vec{r}}{Dt} = \nabla \Phi . \tag{4}$$

The dynamic surface condition is given by Bernoulli's equation,

$$\frac{D\Phi}{Dt} = \frac{1}{2} |\nabla \Phi|^2 - \frac{p}{\rho} - gy . \tag{5}$$

Here y is the elevation of the free surface above the undisturbed water level, g is the acceleration due to gravity (acting vertically downwards), ρ is the fluid density and p is the pressure on the exterior side of the surface. In the presence of surface tension p is given by,

$$p = p_0 + \frac{\tau}{R}, \tag{6}$$

where p_0 is the pressure on the exterior side of the surface, τ is the coefficient of surface tension and R is the radius of curvature given by,

$$R = -\frac{\left[1 + (\partial \eta / \partial x)^2\right]^{3/2}}{\partial^2 \eta / \partial x^2} , \tag{7}$$

with the free surface defined by $y = \eta(x,t)$. The pressure p_0 can be chosen to approximate the effects of wind or a localised pressure on the surface, though it is not used in the calculations.

We assume that the water is deep, satisfying the condition $|\nabla\Phi| \to U$ as $y \to -\infty$. The fluid domain D is chosen to be non-periodic to model the disturbances generated by a submerged cylinder interacting with a uniform stream flow. In this case the fluid surface and the velocity $\vec{u}(x,y,t)$ at the far ends of the domain must be uniform there, satisfying the following boundary condition,

$$\nabla\Phi(x,y,t) \sim (U,0), \tag{8}$$

as $|x| \to \infty$, for $-\infty < y \leq 0$ and $t>0$. To complete the model an initial condition for the free surface is required and given by,

$$\eta(x) = \eta_0(x), \qquad \Phi(x,\eta) = \Phi_0(x,\eta_0), \tag{9}$$

for $t = 0$. The ratio of effects of surface tension with respect to those of gravity for relatively deep water is represented by the Bond number B,

$$B = \frac{\tau}{\rho g L^2}, \tag{10}$$

where L is the depth of submergence of the top of the cylinder, namely *(d-a)*. Here a is the radius of the cylinder and d is the depth of submergence with respect to its centre.

3. Fully nonlinear boundary-integral solver

The boundary value problem is solved using an adapted version of the fully nonlinear potential flow program described by Tanaka *et al.* (1987). The method consists of applying a boundary-integral method to a free surface flow problem, which reduces significantly the computational demand for the calculation of the fluid motion since only surface properties are evaluated. The solution method is based on solving an integral equation that arises from Cauchy's integral theorem for functions of a complex variable. The original numerical scheme is modified for the inclusion of surface tension effects (Jervis 1996) and a dipole (Moreira 2001).

3.1. Integral formulation

The calculation of the free surface velocity $\nabla\phi_w$ becomes relatively simple when applying Cauchy's integral theorem. If we take $z = x + iy$ as the complex equivalent of the position vector $\vec{r} = (x, y)$ for a certain time t, ϕ_w is an analytic function of z. The wave complex potential gradient is defined as,

$$q_w = \frac{\partial \phi_w}{\partial x} - i\frac{\partial \phi_w}{\partial y}, \tag{8}$$

which is also an analytic function of z. On the boundary, z is treated as a function of the parameter ξ and time t. Similarly, taking $Z(\xi,t)$ as the complex equivalent of the surface profile vector $\vec{R} = (x(\xi,t), y(\xi,t))$, q_w can be defined in terms of the tangential and normal gradients of ϕ_w at the surface,

$$\bar{q}_w = \frac{\partial Z}{\partial n_1}\left(\frac{\partial \phi_w}{\partial n_1} + i\frac{\partial \phi_w}{\partial n_2}\right). \tag{9}$$

We assume that the surface contour C that surrounds the fluid domain is smooth, then applying Cauchy's integral theorem leads to,

$$\frac{\partial \phi_w}{\partial n_2} = \frac{1}{\pi}\oint_C \Im\left(\frac{\partial Z/\partial n_1}{Z' - Z}\right)\frac{\partial \phi_w'}{\partial n_2} dn_1' + \frac{1}{\pi}\oint_C \Re\left(\frac{\partial Z/\partial n_1}{Z' - Z}\right)\frac{\partial \phi_w'}{\partial n_1} dn_1', \tag{10}$$

in which $\partial\phi_w/\partial n_2$ can be determined since $\partial\phi_w/\partial n_1$ can be calculated directly. The arclength n_1' is a scalar variable which increases in an anticlockwise sense around the closed contour C. The primed variables Z', $\partial\phi_w'/\partial n_1$ and $\partial\phi_w'/\partial n_2$ are evaluated at points on the surface corresponding to n_1'.

3.2. Inclusion of surface tension effects

Surface tension effects were introduced in the fully nonlinear potential flow solver by Jervis (1996), who investigated the formation of parasitic capillaries on the forward face of steep gravity waves. The implemented model assumes that the surface pressure p is defined by expression (6) and it is related to the inertial and gravitational terms by Bernoulli's equation. As already mentioned, the calculation of the Eulerian time-derivatives of ϕ_w necessitates the computation of higher time derivatives of the surface pressure. The required Lagrangian derivatives of the pressure,

namely Dp/Dt, D^2p/Dt^2, etc., can be deduced directly from expression (6) and are expressed in terms of the surface discretisation parameter ξ. The calculation of the Lagrangian derivatives of p demands the previous estimation of the "total" surface velocity $\vec{u}$ and its material derivatives, namely $D\vec{u}/Dt$, $D^2\vec{u}/Dt^2$, etc. $\vec{u}$ is defined as the sum of a regular part, $\nabla\phi_w$ (which is evaluated numerically using a boundary-integral equation) and a singular part, $\nabla\phi_s$ (which is known for a dipole). $D\vec{u}/Dt$ can be determined since $\vec{u}_t$ is evaluated via a boundary-integral equation. Therefore, from the numerical scheme, both $\vec{u}$ and $D\vec{u}/Dt$ are already known when evaluating Dp/Dt and can be used in the calculation of D^2p/Dt^2 if the required derivatives with respect to ξ are estimated. Since the Taylor series expansion is truncated at the sixth power, there is no need for the estimation of higher order derivatives of pressure.

3.3. Dipole model

The velocity potential for an irrotational flow due to a circular cylinder of radius a held in a stream with uniform velocity c far from the cylinder is given by (Batchelor 1967, p.424),

$$\phi_s(x,y)=U(x-x_0)\left[1+\frac{a^2}{(x-x_0)^2+(y-y_0)^2}+\frac{a^2}{(x-x_0)^2+(y+y_0)^2}\right]. \tag{11}$$

where (x_0,y_0) is the position of the centre of the cylinder. The contour of the cylinder approaches a perfect circle and corresponds to a closed streamline. The disturbances generated at the free surface may deform the closed circular streamline and therefore a perfect circle is no longer obtained. However, for the purpose of our study, we assume that this is sufficiently close to a circle.

3.4. Numerical scheme

Basically the method of solution consists of the following stages. Initially the full potential Φ is known on the surface for each time step. The potential ϕ_s due to the dipole is also defined and subtracted from the surface value of Φ such that the remaining surface wave potential ϕ_w, which has no singularity in the fluid domain, can be used with Cauchy's integral theorem to calculate the velocity $\nabla\phi_w$ on the free surface. Then the potential ϕ_s is added back in and corresponding "total" velocities are evaluated. The inclusion of the singularity necessitates the computation of the partial derivatives with respect to x and y of the velocity potential ϕ_s up to the third derivative, since the time-step criterion uses a Taylor series expansion truncated at the sixth power. Since in our model the dipole is assumed at a fixed position, the partial time derivatives vanish. Once an accurate converged solution is obtained for the full velocity potential Φ on the free surface, the cycle can begin again. Such stages are repeated until either the final time is reached, or the algorithm breaks down. Full details can be found in Dold (1992).

3.5. Accuracy

With the inclusion of surface tension more points are needed to resolve small scale waves accurately. Once again the accuracy of the numerical method relies on the number of surface points employed in the computations. Slightly different surface profiles appear in regions with capillary waves when modelling the same surface with different number of points. The less points used in the computation, the greater are the effects of smoothing on waves with very few points per wavelength. Thus small capillary waves become slightly longer and have smaller amplitudes when poorly resolved.

The numerical scheme follows the calculation points as surface particles, becoming denser in regions where the stream velocity is smallest and thus being "naturally" distributed in greater numbers around the sharp crests of steep waves. However, capillary waves are more likely to have sharp troughs and rounded crests and therefore are not well resolved in a natural way by the numerical scheme. A regridding of the free surface points is then required in order to improve the resolution of such waves.

The numerical scheme is occasionally susceptible to sawtooth numerical instabilities i.e. short scale oscillations of successive points along the surface. In general these sawtooth modes have wavelengths of two consecutive surface points and induce the breakdown of the computation if remained unchecked. Such instabilities feature in most existing numerical schemes that follow the motion of surface gravity waves and were firstly reported by Longuet-Higgins & Cokelet (1976), who employed smoothing techniques to control them.

The numerical code used here often runs without generating sawtooth modes. Otherwise one of the several polynomial formula given by Dold (1992) effectively removes the sawtooth modes that may eventually appear. Although the use of higher order smoothing formulae is less satisfactory than having a numerically stable scheme, this technique is shown to cause little loss of accuracy. The smoothing formula is based on the fitting of high order

polynomials to the surface data, removing any very short wavelength components of the surface variables. Thus waves defined by two or three grid points are selectively removed.

The implications of smoothing on longer wavelengths are very small. In this case gravity is the dominant force and waves defined by a fewpoints may arise only as a result of numerical instabilities. However the inclusion of surface tension may induce the formation of such waves as a physical phenomenon. In this situation smoothing may dissipate these waves numerically. Ripples with only a few calculation points in length have their amplitude significantly reduced by smoothing along with possible numerically generated sawtooth modes. When used, the smoothing algorithm reduces a sharp crest in the same way as a sawtooth instability. This affects directly the roughness of the surface waves, generally postponing the time of wave breaking. Indeed Jervis (1996) described that the introduction of surface tension in the numerical scheme is frequently associated with the appearance of sawtooth numerical instabilities in the surface variables, which was ascribed to the rapid variation of surface quantities with the grid points in the presence of short ripples. In the numerical scheme, the source of these unstable modes resides in the calculation of the capillary wave pressure and its Lagrangian derivatives.

Therefore it is important to use a sufficient number of surface calculation points in order to have any real capillary wave well resolved and thus not being smoothed away by the numerical scheme. The use of smoothing is required since sawtooth modes appear to arise from the calculation of the higher Lagrangian derivatives of pressure, which would eventually cause the breakdown of the computation. For all the computed cases smoothing is minimised as far as possible and a low order formula is used when needed. This proves to be efficient in the removal of unstable modes for long run computations and also gives a slightly larger maximum steepness of surface waves rather than when employing a higher order formula. If wave breaking is expected to occur, smoothing with a low order formula affects the time of breaking less.

The minimum size of the capillary waves that can be accurately calculated by the nonlinear code can be easily estimated e.g. assuming that each wave is defined by at least 5 calculation points and that 600 points are used to discretise a length scale of 12.5 cm, then ripples with wavelengths longer than 1 mm can be accurately resolved in this case. Note that the number of calculation points should increase with the characteristic length scale of the problem if the same resolution is required.

4. Fully nonlinear results

With the introduction of surface tension the linear dispersion relation has a minimum phase speed c_m which defines a region where waves do appear i.e. $U>c_m$. Two real roots then exist and, for $a/d<<1$, linear theory determines accurately the wave properties of the problem. However, if the relation a/d increases, nonlinear effects may become important. If that is the case then the free surface profile is distorted and wave breaking may occur. For a constant d, as a/d assumes larger values, B also increases and thus surface tension effects may postpone wave breaking. Nonlinearity may also affect the free surface profile for values of $U<c_m$. Figure (2) shows the location of the nonlinear cases studied in this section with respect to the phase and group velocity of capillary-gravity waves. The fully nonlinear, unsteady, boundary-integral method introduced in section 3 is here employed taking into account the effects of surface tension.

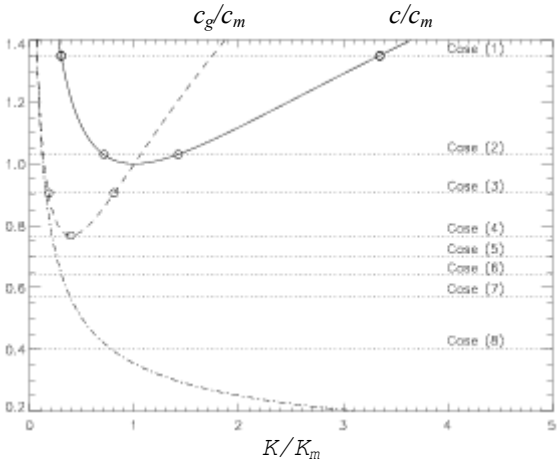

Figure 2. Location of the fully nonlinear results with respect to the phase and group velocity of capillary-gravity waves. The dashed-dotted line represents the group velocity of pure gravity waves. $K_m=B^{-1/2}$; $c_m=(4B)^{1/4}$.

Figures (3a) and (3b) compares quasi-steady nonlinear results with linear steady solutions for cases (1) ($B=0.0754$) and (2) ($B=0.2218$) respectively, where $U>c_m$ (see figure 2). In these cases a flat free surface was used as the initial condition of the boundary value problem. Note that in both cases $a/d=1/10$ and a vertical exaggeration of 10:1 was used. As expected a good agreement was observed between the linear and nonlinear results, with "gravity-like" waves being formed downstream the cylinder and "capillary-like" waves ahead of it, which are visible only in case (2) where surface tension effects become more prominent ($B=0.2218$). In both cases the nonlinear wave amplitudes give accurate

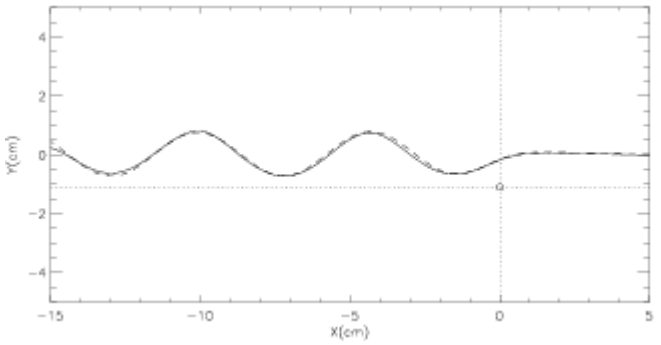

(a)

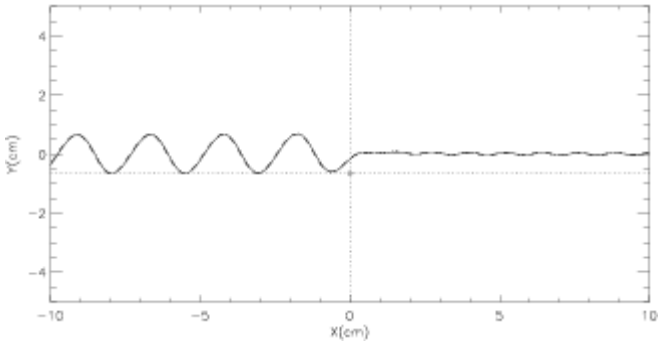

(b)

Figure 3. Comparison between quasi-steady nonlinear results (------) and linear stationary solutions (-- -- --). (a) $B=0.0754$, $U/c_m=1.3494$, $(d-a)=1$cm, $a=0.1111$cm; (b) $B=0.2218$, $U/c_m=1.0301$, $(d-a)=0.583$cm, $a=0.0648$cm. In the cases presented here $a/d=1/10$, $U=-1$, $Fr=0.75$ and $c_m=(4B)^{1/4}$. U and c_m are dimensionless quantities. Vertical exaggeration 10:1.

linear solutions. When the relation a/d is increased to 1/3, keeping U/c_m and B with the same values, nonlinear effects take over and wave breaking occurs in both cases within very short times.

According to linear theory, if the value of U/c_m decreases, such that $U<c_m$, no real steady solution with waves exists for the phase speed, with only a local disturbance being predicted. However two roots exist for the group velocity *if* $c_m>U>c_{gm}$, which may be associated to unsteady waves. Indeed the unsteady nonlinear computed case (3) shows that wave breaking occurs in this region. In fact case (3) has the calculations stopped at $t_{breaking}=4.0$, supposing $B=0.00302$, $a/d=1/3$ and $U/cm=0.9052$ (see figure 4). For case (4), where $B=0.00582$, $a/d=1/3$ and $U/c_m=0.7681$, the time at which breaking occurs has now increased to 10.8. Since B is very small in both cases, surface tension effects are less prominent. Due to the impulsive starting motion some capillary-gravity waves are visible propagating in the $-x$ direction. Waves are also formed ahead of the cylinder but these are "trapped" by the adverse stream flow U, with energy building up there until wave breaking occurs. Note that for case (4), U is very close to c_{gm}.

For $U<c_{gm}$ wave breaking was no longer observed in the unsteady nonlinear computations for constants a/d (=1/3) and U (=-0.3). In fact, as B increases, U/c_m decreases and the capillary-gravity waves generated ahead of the cylinder are no longer "trapped" by the adverse current and now radiate upstream of the cylinder. This feature was observed in cases (5) to (8) for long computational runs (see figure 5), where $B=0.00838$, 0.01206, 0.01885 and 0.0754, respectively. As B increases, surface tension effects become more important. Indeed capillary-gravity waves are formed as the underlying motion is switched on at time $t=0$, generating unsteady waves that propagate in the $-x$ and $+x$ direction. The group velocity of the waves formed downstream of the cylinder is augmented by the following current and radiates away. On the other hand the group velocity of the capillary-gravity waves formed ahead of the cylinder is reduced by the adverse stream flow, as it can be seen from figures (5a) and (5b). As U/c_m keeps decreasing (since B increases), the stream velocity has less effect on the capillary-gravity waves generated until they are totally radiated away in both x directions, as shows figure (5c).

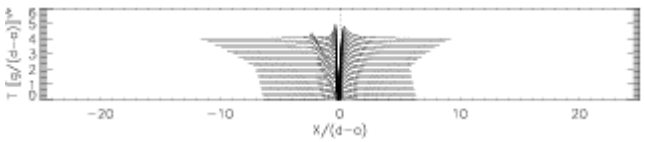

Figure 4. Fully nonlinear result for a uniform stream flow interacting with a submerged cylinder. $B=0.00302$, $U/c_m=0.9052$, $(d-a)=5.0$cm, $a=2.5$cm, $t_{breaking}=4.0$. In this case $a/d=1/3$, $U=-0.3$ and $c_m=(4B)^{1/4}$. U and c_m are dimensionless quantities. Vertical exaggeration 50:1.

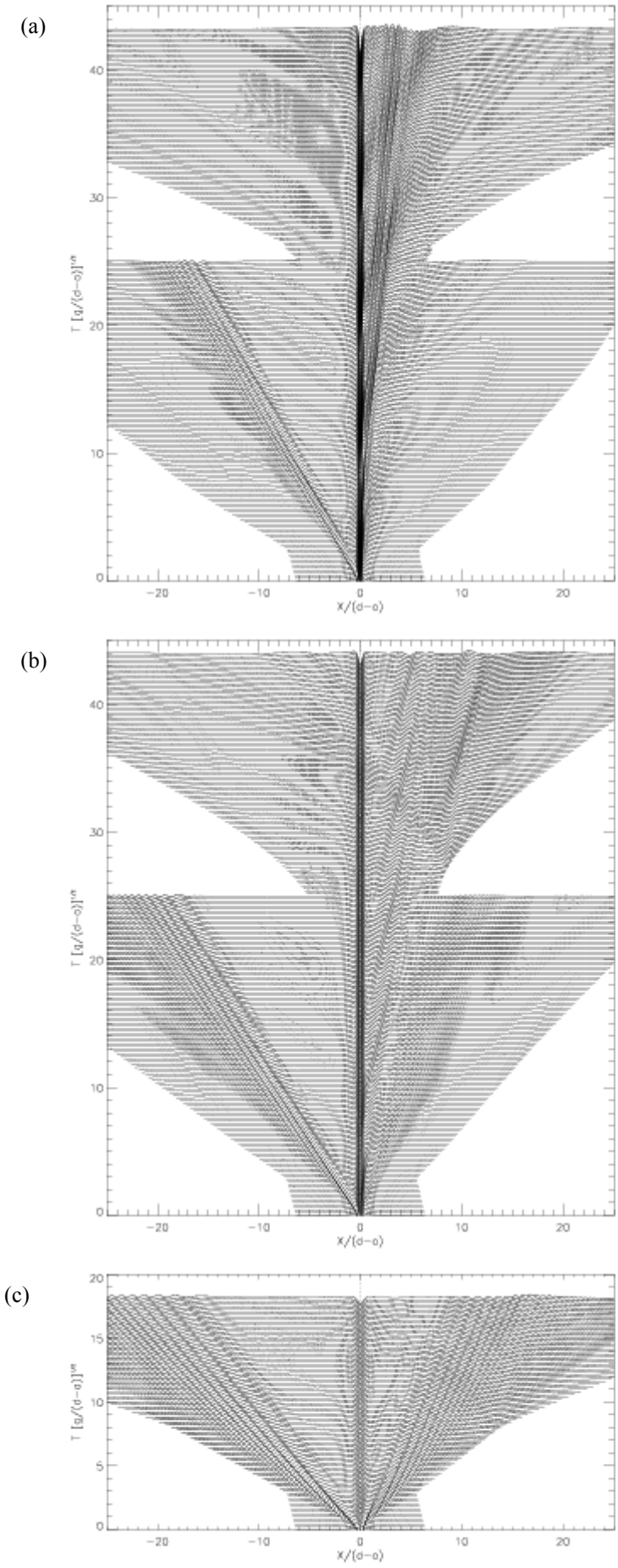

Figure 5. Fully nonlinear results for a uniform stream flow (U=*-0.3*) interacting with a submerged cylinder (*a/d=1/3*). (a) *B=0.00838*, U/c_m=*0.7012*, *(d-a)=3*cm, *a=1.5*cm. (b) *B=0.01885*, U/c_m=*0.5725*, *(d-a)=2*cm, *a=1.0*cm. (c) *B=0.0754*, U/c_m=*0.4048*, *(d-a)=1*cm, *a=0.5*cm. $c_m=(4B)^{1/4}$. U and c_m are dimensionless quantities. Vertical exaggeration 50:1.

6. Summary

The interaction between a free surface flow with surface tension and an approximately circular, horizontal cylinder is investigated. This work was motivated by several authors who had studied the effects of nonlinearity in the classical linear solution given by Lamb (1913), but without considering capillarity. A fully nonlinear model which includes surface tension and a dipole in a stream flow was developed aiming to understand the behaviour of the free surface flow. A linear steady solution including surface tension effects was derived and employed as the initial condition of the nonlinear model. For sufficiently small values of a/d, a good agreement between the quasi-steady nonlinear numerical results and the linear steady solutions is obtained for both pure gravity and capillary-gravity waves. However, as the relation a/d increases, nonlinearity starts to play an important role. For pure gravity waves, the fully nonlinear results show that waves become "steeper", with sharper crests and shorter wavelengths, with wave breaking occurring when larger values of a/d are imposed.

With the introduction of surface tension, the numerical simulations have shown that wave breaking also occurs for sufficiently large values of a/d i.e. $a/d>1/3$, but now this also depends on the Bond number B. As B increases, surface tension effects become more prominent; capillarity can then significantly reduce the steepness of the free surface disturbances when it precludes the formation of steady waves. For $U>c_{gm}$ wave breaking was observed in all the computed cases when the inequality $a/d<<1$ was not satisfied. For $U<c_{gm}$, an interesting feature was found: capillary-gravity waves are formed upstream the cylinder. According to linear theory, only a local disturbance which decays rapidly to zero with distance from the centre of the cylinder should happen in this case. However in an initial value problem waves can radiate away. As U/c_m decreases, with values smaller than the minimum group velocity c_{gm}, waves of all frequencies are radiated upstream and downstream. Then the nonlinear result approaches the linear steady solution of a local disturbance at the free surface.

7. Acknowledgement

I am grateful for the guidance and useful discussions with Prof. D.H.Peregrine of the School of Mathematics, University of Bristol. I acknowledge the financial support through CAPES, the brazilian agency for post-graduate education, and Fluminense Federal University.

8. References

Dagan, G., 1971, "Free-surface gravity flow past a submerged cylinder." J. Fluid Mech. 49, pp. 179–192.

Dold, J.W., 1992, "An Efficient Surface-Integral Algorithm Applied to Unsteady Gravity Waves." J. Comp. Phys., v. 103, pp. 90-115.

Jervis, M.T., 1996, "Some Effects of Surface Tension on Water Waves and Water Waves at a Wall." PhD thesis, University of Bristol, U.K.

Lamb, H., 1932, "Hydrodynamics." 6th ed., Cambridge Univ. Press.

Longuet-Higgins, M.S. & Cokelet, E.D., 1976, "The deformation of steep surface waves on water. I. A numerical method of computation." Proc. R. Soc. Lond., A 350, pp. 1-26.

Moreira, R.M., 2001, "Nonlinear interactions between water waves, free surface flows and singularities." PhD thesis, University of Bristol, U.K.

Tanaka, M., Dold, J.W., Lewy, M. & Peregrine, D.H., 1987, "Instability and breaking of a solitary wave." J. Fluid Mech. 185, pp. 235–248.

Tuck, E.O., 1965, "The effect of non-linearity at the free surface on flow past a submerged cylinder." J. Fluid Mech. 22, pp. 401–414.

9. Copyright notice